Droptower Impact Testing & Modeling of 3D-Printed Biomimetic Hierarchical Composites

Grace Xiang Gu[1], Steven Kooi[2], Alex J. Hsieh[23], Chian-Feng Yen[3], and Markus J. Buehler[4]

[1] Laboratory for Atomistic and Molecular Mechanics (LAMM), Department of Mechanical Engineering, Massachusetts Institute of Technology, Cambridge, MA 02139, USA
[2] Institute for Solider Nanotechnologies, Massachusetts Institute of Technology, Cambridge, MA 02139, USA
[3] US Army Research Laboratory, Aberdeen Proving Ground, MD 21005, USA
[4] Laboratory for Atomistic and Molecular Mechanics (LAMM), Department of Civil and Environmental Engineering, Massachusetts Institute of Technology, Cambridge, MA 02139, USA

Abstract

Inspired by the hierarchical designs of natural materials, this paper highlights the use of 3D-printing as a plausible pathway to discern and differentiate material attributes critical to desirable impact properties. A comprehensive study was focused on the influence of three different hierarchical designs derived from a nacre-like architecture, where two base materials varying vastly in properties were used to evaluate the low-velocity impact on 3D-printed hierarchical materials. The work presented here develops a numerical model to characterize the failure modes and damage behavior of various hierarchical materials organized in different configurations. The finite element software LS-DYNA® is used where force-displacement responses and damage patterns obtained from simulation are compared with experimental results obtained from drop tower impact tests. This study clearly demonstrates that the emerging 3D-printing technology can enable rapid prototype towards hierarchical ductile/brittle hybrid designs for future impact resistant materials.

Introduction

Polymers unlike glass and ceramics are viscoelastic materials and exhibit a wide range of mechanical deformation behavior. For instance, polycarbonate, PC, is ductile while poly (methyl methacrylate), PMMA, is hard and brittle; both materials are currently used in a variety of commercial, military and security protection applications. PC has excellent impact resistance properties, thus is the choice of material for use in safety lenses, goggles, transparent face shields, as well as windshields for vehicles. However, PC not only has very poor resistance to abrasion and many organic solvents but also is very notch sensitive and prone to physical-aging, both detrimental to impact performance. In addition, the embrittlement, as a result of a ductile-to-brittle transition, noticeably for plate thickness greater than about 5-6 mm, precludes the use of a PC monolith in the design of impact-protective structure components above the threshold thickness. On the other hand, PMMA upon impact exhibits brittle mode of deformation, where a fractured cone along with radial cracks are typically generated at the point of impact, which resemble the Hertzian cracks formation. Despite its inherent brittle nature, PMMA exhibits a greater dynamic strain-rate hardening characteristic than PC [1, 2].

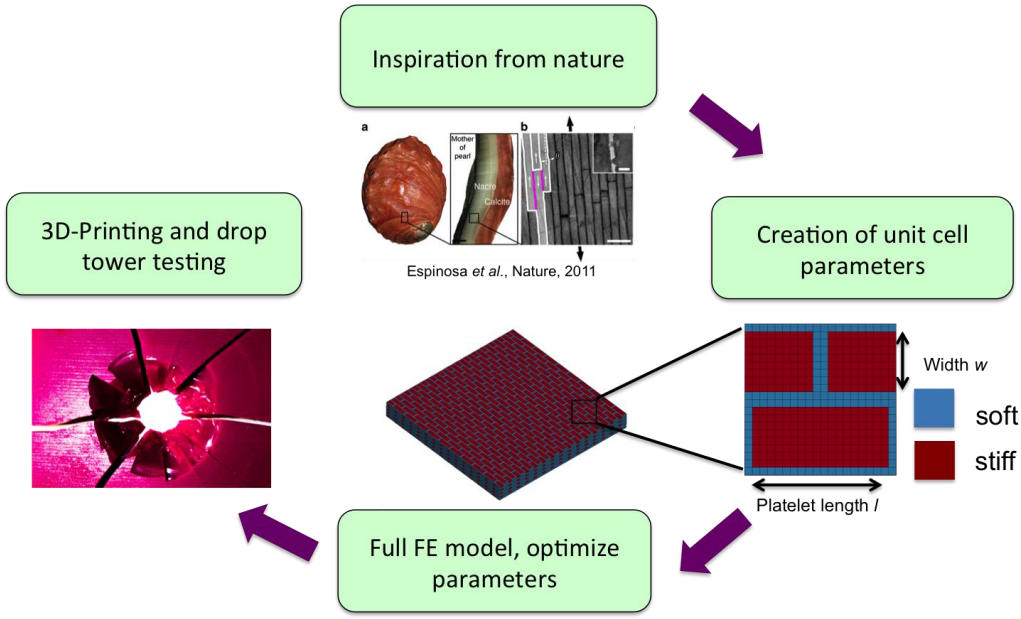

Figure 1: Methodology includes creating a material using inspiration from nature, modeling using LS-DYNA, 3D-printing of various designs, and performing impact measurements via droptower impact testing.

For glassy polymers, the mode of deformation typically involves either crazing or shear yielding, leading to a brittle or ductile mode of failure, respectively. However, altering the state of stress can give rise to a change in the mode of failure. For example, PC can exhibit brittle failure by simply increasing the plate thickness, due to the presence of a triaxial-stress state (plane strain condition) favoring craze formation. On the other hand, a typically brittle PMMA can exhibit ductile deformation as observed in thin monolithic films or in thin layers in coextruded multi-layered (i.e. PC/PMMA) composite [3, 4], wherein PMMA is in plane stress and exhibits shear yielding upon deformation. In addition, PMMA, under confinement, also exhibits complete suppression of radial cracks formation [5]. Recently, there have been significant interests in the research and development of plausible pathways, particularly via a biomimetic approach to further optimization of fracture toughness and mode of failure upon impact. One example is the design and fabrication of *de novo* synthetic materials that aim to utilize the deformation and hardening mechanism of biological materials such as bone or nacre, which is an active area of research in mechanics of materials [6]. In this study, we exploit and highlight the role of hierarchical designs seen in natural composites such as nacre or mother of pearl, and the goal is to discern and differentiate the material attributes, which are critical to dynamic impact performance. It is envisioned that 3D-printing could be an enabling materials technology capable of imitating these designs, not achievable by the current state-of-the-arts in polymer processing [7].

From the materials perspective, the hierarchical designs via 3D printing could serve to guide the design with optimized material properties including impact resistance, toughness, and density. To mimic the unique brick-and-mortar architecture in nacre, which also consists of two vastly different materials [6, 8, 9], 3D nacre-like designs are created from a unit cell and simulations using LS-DYNA are performed. In 3D printing, materials can be integrated through a combination of a soft and a stiff material of varying compositions and scales, where the soft material exhibits a ductile failure mode, whereas a brittle mode of failure is typically seen in the

stiff material. In this work, we investigate 3D printing of different configurations of select model designs and their corresponding impact performance under droptower testing. This includes a comparison of impact resistance and failure patterns among the different hierarchical designs. A schematic illustrating this general methodology is portrayed in Fig.1. These results will provide a better understanding with respect to the attribute of hierarchy for use in the design of ductile/ brittle hybrids, which is unparalleled to the current materials technology, towards better optimization of commercial materials such as PC and PMMA.

Experimental results

Additive manufacturing with two types of base materials was executed. The two base materials used in this study were 3D-printed using proprietary Stratasys photopolymers, Veromagenta and Tangoblackplus. The Veromagenta grade is the comparatively stiffer material, whereas the Tangoblackplus grade is more flexible and rubber-like. In this paper, these will be referred to as stiff and soft materials, respectively. Material testing of the two base materials and hybrid materials was done using low-velocity impact tests. The test procedures and results are discussed in what follows.

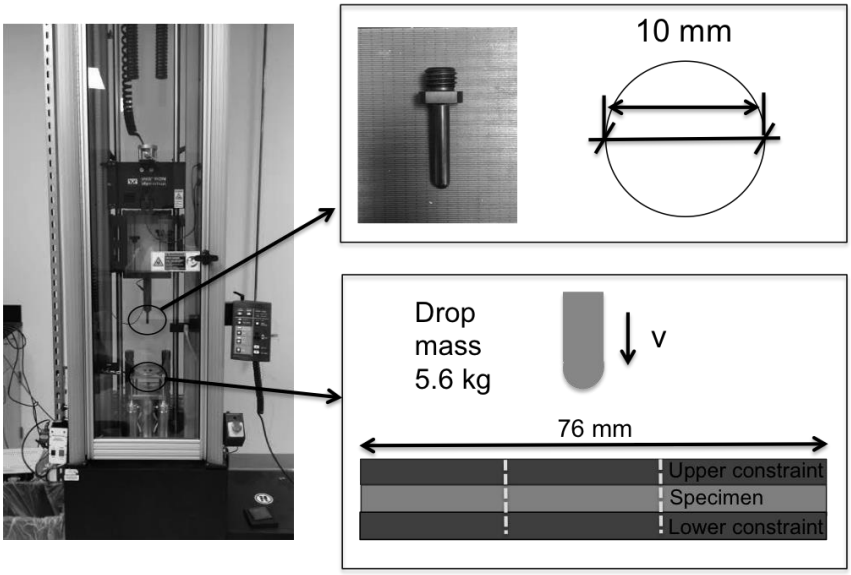

Figure 2: Droptower setup describing impactor dimensions, sample positions, and constraints in the system

Monolithic material low-velocity droptower impact tests

The droptower test setup and associated parameters are illustrated in Fig. 2. Square specimens (75 mm by 75 mm by 8 mm) of the two disparate 3D-printed materials were chosen for testing. A side length of 75 mm was chosen due to the fixture constraints of the test setup. A thickness below 8 mm could not be adequate to acquire reliable data of the threshold failure load values, where 50 percent of the specimens would break. The specimens are held by a circular clamp of diameter 38 mm in the fixture of an Instron drop weight impact tester. The hemispherical impactor is 10 mm in diameter and attached to a mass of 5.6 kg, which is then dropped at a set height to perform the impact test. The height is used to determine the velocity at impact $\left(v = \sqrt{2gh}\right)$.

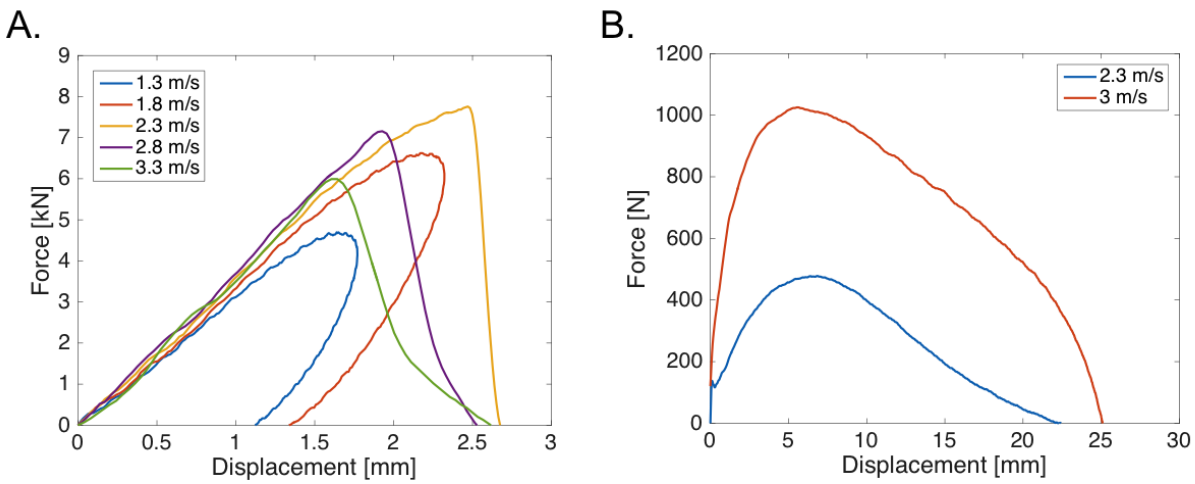

Figure 3: A. Force displacement curves for the stiff material at various velocities. B. Force displacement curves for the soft material at various velocities.

The contact force is measured by an Instron load cell, which is located on top of the impact tup, and the velocity is recorded by photoelectric diodes. The specimen is first placed on a flat surface in the clamping area, the circular clamp then drops onto the specimen, securing the specimen. Subsequently, the impactor is dropped from the desired height, which dictates the velocity at impact. After impact, the clamp automatically returns up, and the specimen is recovered from the fixture for damage observation and analysis. The force-displacement curves at various velocities of the impactor for the two materials are shown in Fig 3. For the stiff material, velocities below 2.3 m/s did not penetrate the specimen (rebounded), while velocities above 2.3 m/s penetrated. For the soft material, velocities below 3 m/s did not penetrate the specimen; instead the impactor slowly went downwards into the material and created a large deformation. Different damage patterns were noted which are shown in Fig. 4. The stiff materials exhibit brittle mode of cracks initiation and propagation, where the failure pattern resembles the radial cracking typically seen in commercial glassy PMMA. In contrast, the soft materials reveal a plug failure pattern strongly indicative of a ductile failure, similar to those seen in elastomers. Given the congruence characteristic of failure modes, it is envisioned that 3D-printing could be a plausible pathway to model and guide the design of commercial materials for better fabrication into hierarchical hybrid structures.

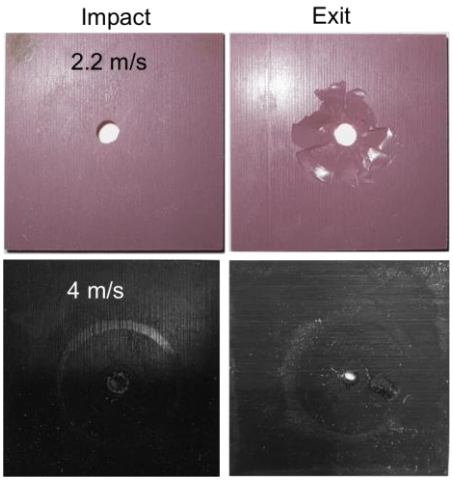

Figure 4: Representative damage patterns observed for monolithic stiff (top) and monolithic soft (bottom) on the impact and exit sides.

Hybrid materials characterization

Specimen dimensions for the hybrid materials are the same as that of the base materials, however, for hybrid laminates the specimens are made up of the same ply but in different stacking sequences. The ply is composed of unit cells shown in Fig. 5 where there is a combination of soft and stiff materials organized in a brick-and-mortar geometry repeated 20 times in each in-plane direction. For each ply, this same unit cell is repeated in plane and the overall dimensions of the hybrid specimens are 75 mm by 75 mm by 1 mm (Fig. 5). Eight copies of this ply are then manipulated to create three different configurations. The first configuration is called "Repeating" design and is uniform through its thickness, in which the first layer is repeated eight times ($[0_8]_T$), where T stands for total. The second configuration is "Rotated" pattern, $[0/90]_{4,}$ in which the layers are laid up following a 90° rotation in alternate layers. The third configuration is "Staggered" pattern in which two layers are displaced from each other by 1 mm in each in-plane direction; these two layers are then repeated four times to build up the laminate.

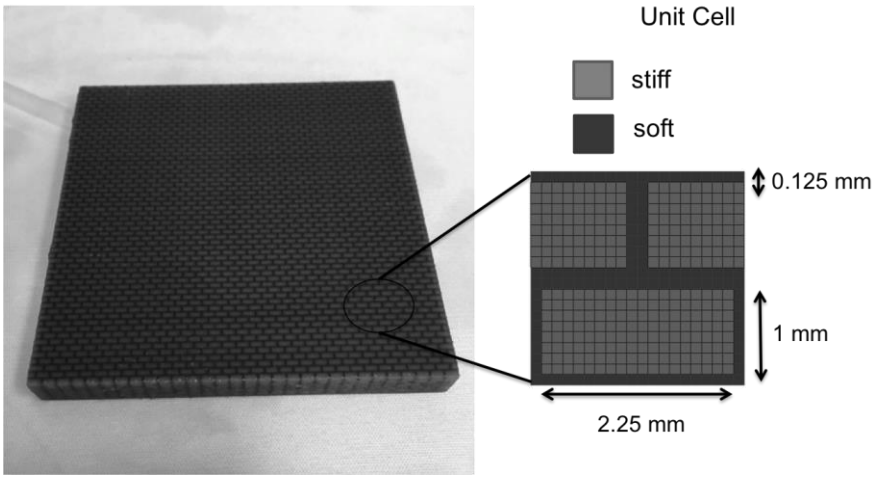

Figure 5: Unit cell parameters for each ply layer. Unit cell is composed of both the soft and stiff materials.

The various hybrid specimens are impacted at a fixed velocity of 2.3 m/s and the damage patterns are compared (Fig. 6). For the Rotated design, the impactor did not result in complete perforation in the test specimen. In fact, the Rotated design had the least damage compared to the Repeating and Staggered designs. The force-displacement curves and velocity-time curves for the three configurations are shown in Fig. 6. In the rotated design the velocity vs. time data reveals that the material was able to attenuate the impact velocity to zero at the end of the test. It is of note that for all hybrid specimens the force-displacement data reveal a step change or discontinuity as impact progresses, which presumably are a result of the onset of microcracks formation, thus, could be strongly indicative of the benefit of hierarchical designs.

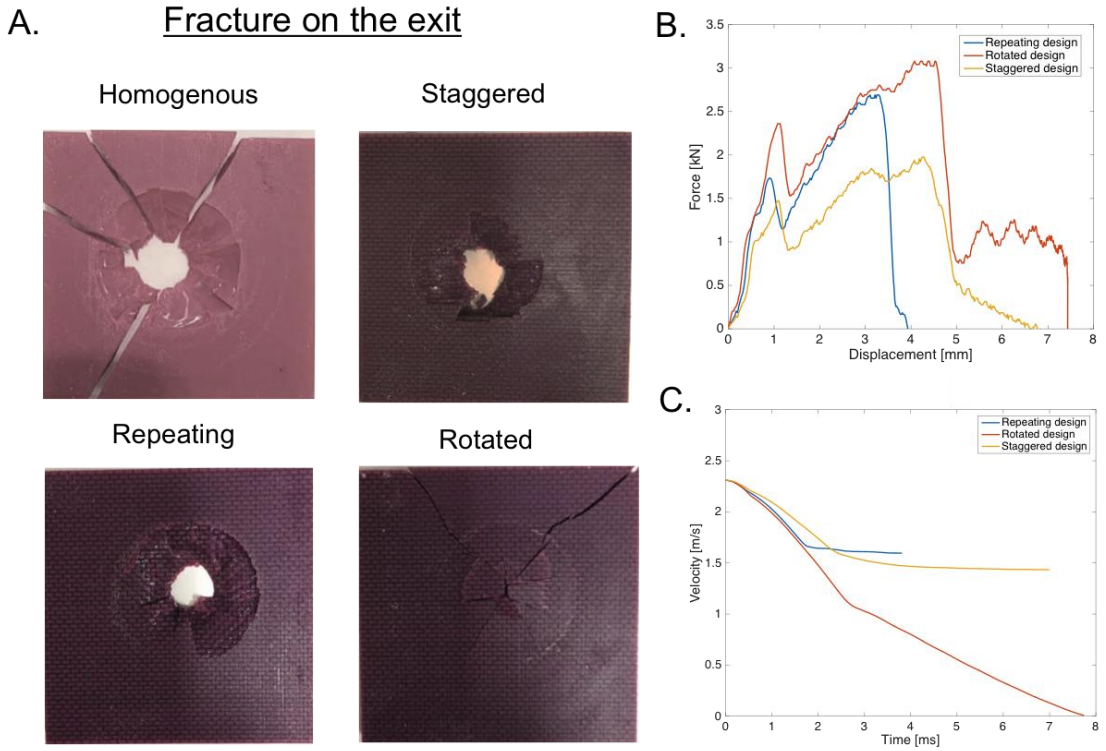

Figure 6. A. Fracture patterns for the various configurations compared to the monolithic stiff material. B. Force displacement curves for the various hierarchical design configurations. C. Velocity over time curves for the various configurations, where rotated design allowed the velocity at impact to decrease to 0 m/s.

Numerical Results

Model parameters

The dropweight impact tests on hierarchical designs were simulated through a commercially available three-dimensional nonlinear dynamic finite element code, LS-DYNA. The development of the model involved defining geometry, input of material properties, creating the mesh, and setting boundary conditions. Three main parts are used in the simulation: impactor, stiff material, and soft material. The stiff and soft material are hierarchically architected in a brick-and-mortar design. These designs are then stacked into different sequences: repeating, rotated, and staggered designs as mentioned in the experimental section. The model set-up and designs along with the mesh of the repeating design are shown in Fig 7. A circular

geometry is used for all cases with a diameter of 38 mm and a thickness of 8 mm, matching the experimental set up dimensions of the impacted region. The model is circular because of the circular clamped conditions. The boundary conditions of the above model are as follows: fixed in all directions and rotations along the circular edge. Symmetry boundary conditions are applied along the symmetry edge and the impactor is constrained in all directions except for z-direction.

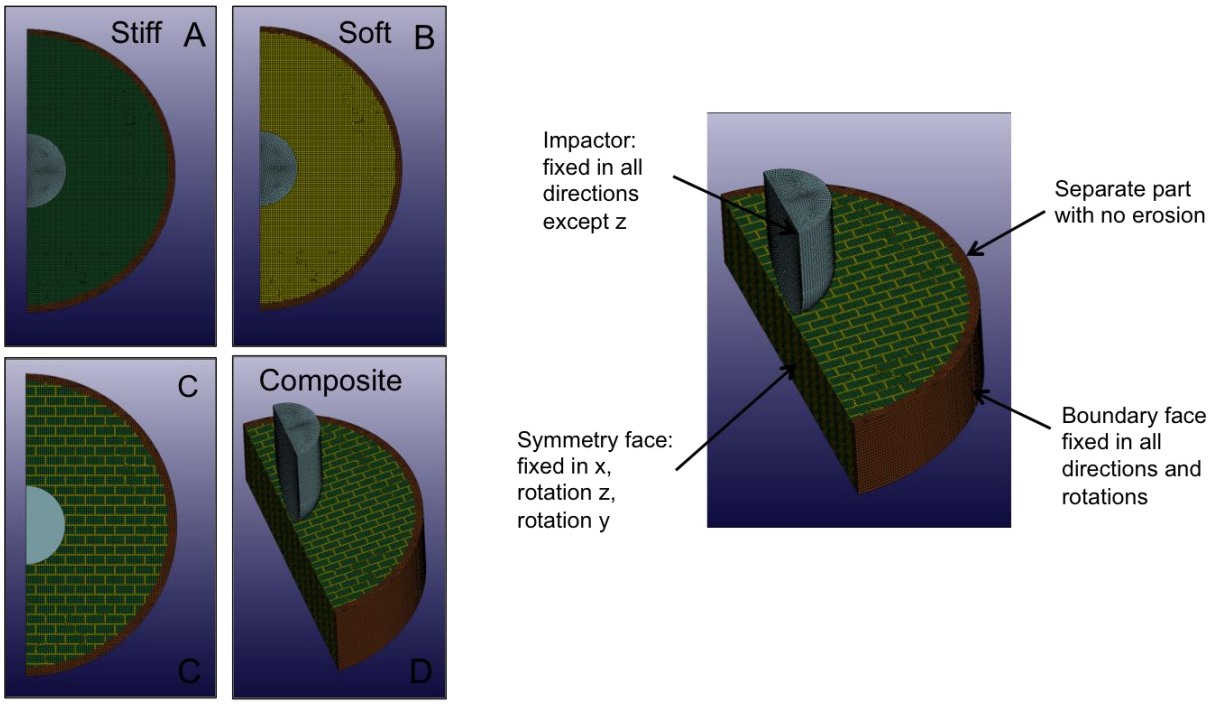

Figure 7: Simulation set up and boundary conditions to match droptower experiments. The composite and base material geometry and mesh are illustrated.

Impactor is modeled as a rigid material (RIGID). Stiff material is modeled as an elastic-plastic material, and soft material is modeled as a hyperelastic material; their mechanical properties are listed in Table 1 and Table 2. The material models for the stiff material are obtained through Reference [10], a hard acrylic material. The material model used for the soft material is the Arruda-Boyce Rubber model. For this model, the bulk modulus and shear modulus is obtained from the tensile testing stress-strain curve of the 3D-printed material. The much higher Young's modulus and tensile strength of the steel impactor than the other materials implies that the impactor can be simplified to be a rigid body. ADD EROSION is added to each material model with failure determined by maximum stress for the stiff material and effective strain for the soft material. This feature is not added in the outer boundary part of the model because the boundary failure is not physical. During impact, the dynamic contact, which occurred between the rigid impactor and the material, was accounted for using the LS-DYNA EROSION contact card. Erosion single surface contact has been assigned between the impactor and composite. Stiffness-based hourglass control is used to inhibit nonphysical, zero-energy modes of deformation. Total energy and hourglass energy is compared to make sure hourglass energy is low enough. The termination time, computational time step, and output time step were specified in the control cards of LS-DYNA. The output is in the form of d3-plots, where damage results and stress/strain fields are analyzed using the LS-PrePost® postprocessor.

Table 1. Elastic-plastic material model used for stiff material

	Density	Young's modulus	Yield stress	Poisson's ratio	Failure stress
Value	0.001	2740	45	0.3	75
Units	g/mm^3	MPa	MPa	--	MPa

Table 2. Arruda-Boyce rubber material model used for soft material

	Density	Bulk modulus (K)	Shear Modulus (G)	Poisson's ratio	Failure strain
Value	0.001	150	3	0.49	1.0
Units	g/mm^3	MPa	MPa	--	--

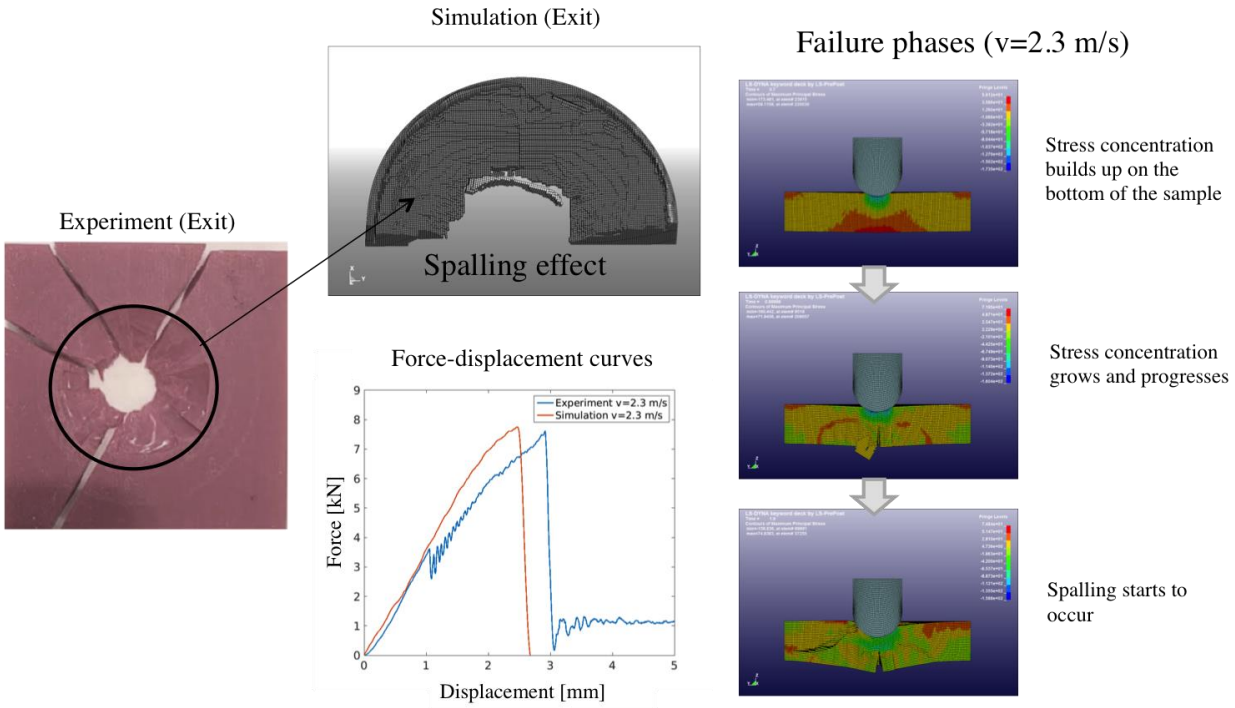

Figure 8: Simulation of stiff material reveals the same failure mechanism of spalling as the experiment. Force displacement from simulation agrees well with experiment. Failure phases show the splitting off of material from the middle to the sides.

Results of numerical model

The mechanical response of the stiff material is shown in Fig. 8. In the experiment, spalling or perforation occurred which caused material to chip away from the bottom of the impact surface. Using the material model proposed earlier, simulation was able to achieve the spalling effect seen in experiment. The force-displacement response also agreed well with experiments. As impact progresses, the material went through various failure phases, starting

with stress concentration at the bottom of the sample. This causes material to erode starting from the bottom and elements starts to split apart. Subsequently, this new configuration caused a new stress concentration to occur around the impact area, which eventually led to perforation of the bottom elements. The soft material simulation response is shown in in Fig.9. Similar to experiment, as the impactor is released, it slowly deforms and stretches the material to high displacement. The mismatch in the initial slope of the force-displacement curve may be due to dynamic rate-effect in the soft material, which was not considered during the current simulation and will be considered in the future using split Hopkinson bar test data. The effective strain fields are also shown for the soft material, which allows us to observe the strain patterns and the damage progression over time. Improved characterization and modeling of material properties would be useful as these are essential for validation of experimental data. In the future, correlation of simulation results with experimental data will be conducted by taking into account rate effects, and these material models will be used to simulate the entire composite response.

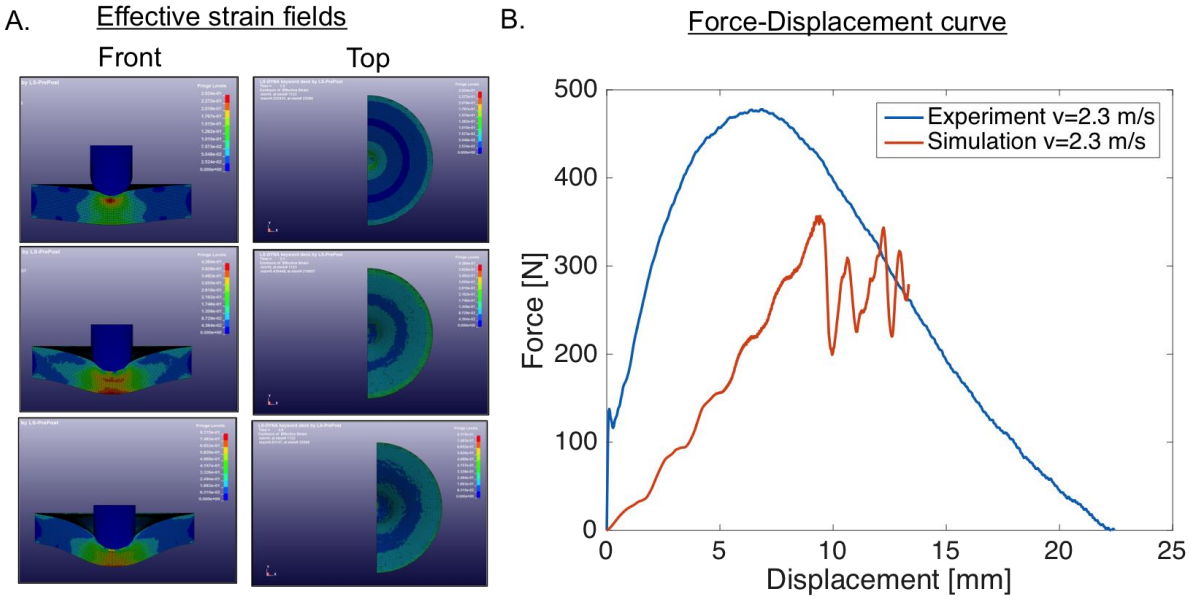

Figure 9: A. Soft material failure mechanisms and effective strain fields. B. Comparison of force-displacement curve between experiment and simulation.

Conclusions and future work

Natural materials demonstrate that adding hierarchy can create stunning materials that are stronger and tougher than its constituents. We studied nacre-like designs using two base materials that are vastly different in properties and structured them in a ply with a nacre-like architecture. These plies are then stacked in different sequences such as repeating, rotated, and staggered. Impact test of 3D-printed designs were conducted in a drop tower setup. From experimentation, we compared the failure patterns observed in each of the designs and noticed that our rotated design performed superior to the monolithic and other studied designs. Additionally, force displacement curves from experiments are compared with those calculated from the finite element model for the two base materials. Future work includes a more thorough material characterization of the 3D-printing materials to better predict damage and composite response in our numerical model. Additionally, optimization of the brick-and-mortar patterns will be done in the future to create more impact resistant materials. Impact response of laminates

will be simulated using FEM to predict damage in the exit surface, high stress concentrations, and failure mechanisms. This combination of 3D-printing, droptower impact testing, and FEA simulations can provide better understanding of material attributes critical towards next generation impact resistant materials.

References

[1] Hsieh, A. J., DeSchepper, D., Moy, P., Dehmer, P. G., and Song, J. W., 2004, "The effects of PMMA on ballistic impact performance of hybrid hard/ductile all-plastic-and glass-plastic-based composites," U.S. Army Research Laboratory Technical Report, ARL-TR-3155.
[2] Moy, P., Weerasooriya, T., Chen, W., and Hsieh, A., "Dynamic stress-strain response and failure behavior of PMMA," Proc. ASME 2003 International Mechanical Engineering Congress and Exposition, American Society of Mechanical Engineers, pp. 105-109.
[3] Hsieh, A. J., and Song, J. W., 2001, "Measurements of ballistic impact response of novel coextruded PC/PMMA multilayered-composites," Journal of reinforced plastics and composites, 20(3), pp. 239-254.
[4] Sharma, R., Boyce, M. C., and Socrate, S., 2008, "Micromechanics of toughening in ductile/brittle polymeric microlaminates: Effect of volume fraction," International Journal of Solids and Structures, 45(7), pp. 2173-2202.
[5] Rittel, D., and Brill, A., 2008, "Dynamic flow and failure of confined polymethylmethacrylate," Journal of the Mechanics and Physics of Solids, 56(4), pp. 1401-1416.
[6] Espinosa, H. D., Rim, J. E., Barthelat, F., and Buehler, M. J., 2009, "Merger of structure and material in nacre and bone–Perspectives on de novo biomimetic materials," Progress in Materials Science, 54(8), pp. 1059-1100.
[7] Gu, G., Su, I., Sharma, S., Voros, J., Qin, Z., and Buehler, M. J., 2016, "3D-printing of bio-inspired composites," Journal of biomechanical engineering.
[8] Kakisawa, H., and Sumitomo, T., 2011, "The toughening mechanism of nacre and structural materials inspired by nacre," Science and Technology of Advanced Materials, 12(6), p. 064710.
[9] Barthelat, F., and Espinosa, H., 2007, "An experimental investigation of deformation and fracture of nacre–mother of pearl," Experimental mechanics, 47(3), pp. 311-324.
[10] Ramakrishnan, K., and Shankar, K., 2013, "Experimental and numerical analysis of low-velocity impact of plastic laminates," Fatigue & Fracture of Engineering Materials & Structures, 36(11), pp. 1153-1163.